GDCh

Research Articles

Angewandte
Chemie
International Edition
www.angewandte.org

Analytical Methods **Hot Paper**

Real-Time Monitoring of Dynamic Microbial Fe(III) Respiration Metabolism with a Living Cell-Compatible Electron-Sensing Probe

Na Chen[+], Na Du[+], Wenjie Wang, Tiangang Liu, Quan Yuan,* and Yanbing Yang*

Abstract: Monitoring microbial metabolism is vital for biomanufacturing processes optimization. However, it remains a grand challenge to offer insight into microbial metabolism due to particularly complex and dynamic processes. Here, we report an electron-sensing probe Zn_2GeO_4:Mn@Fe^{3+} for real-time and dynamic monitoring of Fe(III) respiration metabolism. The quenched persistent luminescence of Zn_2GeO4:Mn@Fe^{3+} is recovered when Fe^{3+} accepted electrons from the dynamic Fe(III) respiration metabolism, enabling the real-time monitoring of microbial metabolism. The probe shows the capability to verify the role of related biomolecules in microbial Fe(III) respiration metabolism, to track the dynamic Fe(III) respiration metabolic response to environmental stress and microbial co-culture interactions. Furthermore, the Zn_2GeO_4:Mn@Fe^{3+} probe provides guidance for improving biosynthesis efficiency by monitoring Fe redox recycling in microbial co-culture.

Introduction

As the center of microbial life, microbial metabolism provides necessary energy and building blocks for cellular activities.[1] Metabolism processes that couple elemental reactions, such as microbial photosynthesis and respiration, perform critical functions in driving major global elemental cycles.[2] Currently, microbial metabolism has been widely applied in the production of fine chemicals. For example, high value-added biofuels and pharmaceuticals can be biomanufactured with microbial cell factories through engineered metabolic pathways.[3] Monitoring the microbial metabolism processes in real-time could facilitate the under-

standing of metabolic mechanism and guide biomanufacturing pathways optimization.[4] Consequently, it is of vital importance to develop efficient microbial metabolism monitoring methods to understand the intrinsic physiological metabolism processes.

Microbial metabolism is a series of biochemical reactions that include numerous decomposed and synthesized chemical molecules.[5] Various substances such as nucleic acids, proteins and chemical molecules are involved in the metabolism processes.[6] In addition, metabolism intermediates are included within different metabolic pathways in microorganism. The metabolism complexity is prominently increased due to the interconnected interactions between and within intricate metabolic pathways in microorganism.[7] Additionally, microorganism requires to dynamically regulate the metabolic pathways by generating a series of adaptive and protective responses to environmental stresses, and this dynamic process further increases the metabolism complexity.[8] In this regard, it remains a grand challenge to monitor microbial metabolism processes in real-time due to the extraordinary complexity of metabolic systems.

Fe(III) respiration, also called dissimilatory Fe(III) reduction, is one of the earliest forms of microbial respiration that sustains microbial growth.[9] Typically, Fe(III) respiration bacteria are represented by *Shewanella* and *Geobacter* species.[9c] In the Fe(III) respiration metabolism process, external Fe^{3+} can be reduced to Fe^{2+} by electrons that are transmitted across the cell membrane of microorganisms.[10] Consequently, the design of a probe with the capability to detect Fe^{3+}/Fe^{2+} ratio is expected to be an efficient approach to monitor electron transfer processes of dynamic Fe(III) respiration metabolism. Various techniques including fluorescence,[11] colorimetry,[12] electrochemistry,[13] atomic absorption spectrometry and inductively coupled plasma-mass spectrometry have been utilized for Fe^{3+} and Fe^{2+} detections.[14] Currently, luminescent sensing techniques based on afterglow materials have attracted great attention in analyzing complex biosystems due to the ability to eliminate autofluorescence interference.[15] Consequently, developing afterglow probe with the ability to detect Fe^{3+}/Fe^{2+} is promising in monitoring the complex and dynamic metabolism processes.

Here, we report an electron-sensing afterglow probe Zn_2GeO_4:Mn@Fe^{3+} (ZGO:Mn@Fe^{3+}) for real-time and dynamic monitoring of Fe(III) respiration metabolism. *Shewanella putrefaciens* CN32 (*S. putrefaciens*) with Fe(III) respiration metabolism is selected as the research model. The quenched persistent luminescence of ZGO:Mn@Fe^{3+} is recovered when Fe^{3+} accepted electrons from the dynamic

[*] N. Chen,[+] N. Du,[+] Prof. T. Liu, Prof. Q. Yuan, Prof. Y. Yang
College of Chemistry and Molecular Sciences, Key Laboratory of Combinatorial Biosynthesis and Drug Discovery, Ministry of Education and School of Pharmaceutical Sciences
Wuhan University, Wuhan 430072 (P. R. China)
E-mail: yuanquan@whu.edu.cn
yangyanbing@whu.edu.cn

W. Wang, Prof. Q. Yuan
Molecular Science and Biomedicine Laboratory (MBL), Institute of Chemical Biology and Nanomedicine, State Key Laboratory of Chemo/Biosensing and Chemometrics
College of Chemistry and Chemical Engineering, Hunan University
Hunan University, Changsha 410082 (P. R. China)

[+] These authors contributed equally to this work.

Fe(III) respiration metabolism processes of *S. putrefaciens*, thus enabling the monitoring of Fe(III) respiration metabolism. The electron-sensing probe ZGO:Mn@Fe^{3+} could be utilized to verify the role of related biomolecules in microbial Fe(III) respiration metabolism as well as to track the metabolic response of *S. putrefaciens* to environmental stresses. Additionally, the metabolic processes involved in microbial co-culture could be monitored with ZGO:Mn@Fe^{3+} probe in real-time. Consequently, based on the excellent performance in metabolic processes monitoring, the electron-sensing probe ZGO:Mn@Fe^{3+} provides guidance for microbial co-culture biosynthesis yields optimization. The reported electron-sensing probe offers an efficient platform for monitoring complex and dynamic microbial metabolism, facilitating metabolic pathways optimization in biomanufacturing.

Results and Discussion

S. putrefaciens, as one of the earliest dissimilatory metal-reducing bacteria, can thrive through Fe(III) respiration metabolism in which electrons from cytoplasm can be transferred to extracellular minerals through metal reducing extracellular electron transfer pathways (Figure 1a).[16] ZGO:Mn nanorods, as a kind of afterglow luminescence nanomaterials, exhibit a band gap ($E_{ZGO:Mn}$) of 4.75 eV as determined by UV/Vis diffuse reflectance spectra (DRS) (Figure 1b and Figure S1 and S2).[17] The energy level diagrams of ZGO:Mn nanorods and Fe^{3+}/Fe^{2+} were depicted in Figure 1c.[17,18] As shown in Figure 1c, the persistent luminescence of ZGO:Mn nanorods at 536 nm originates from the $^4T_1(G)\rightarrow^6A_1(S)$ transition of Mn^{2+} luminescence center.[13] The reduction Fermi energy level of
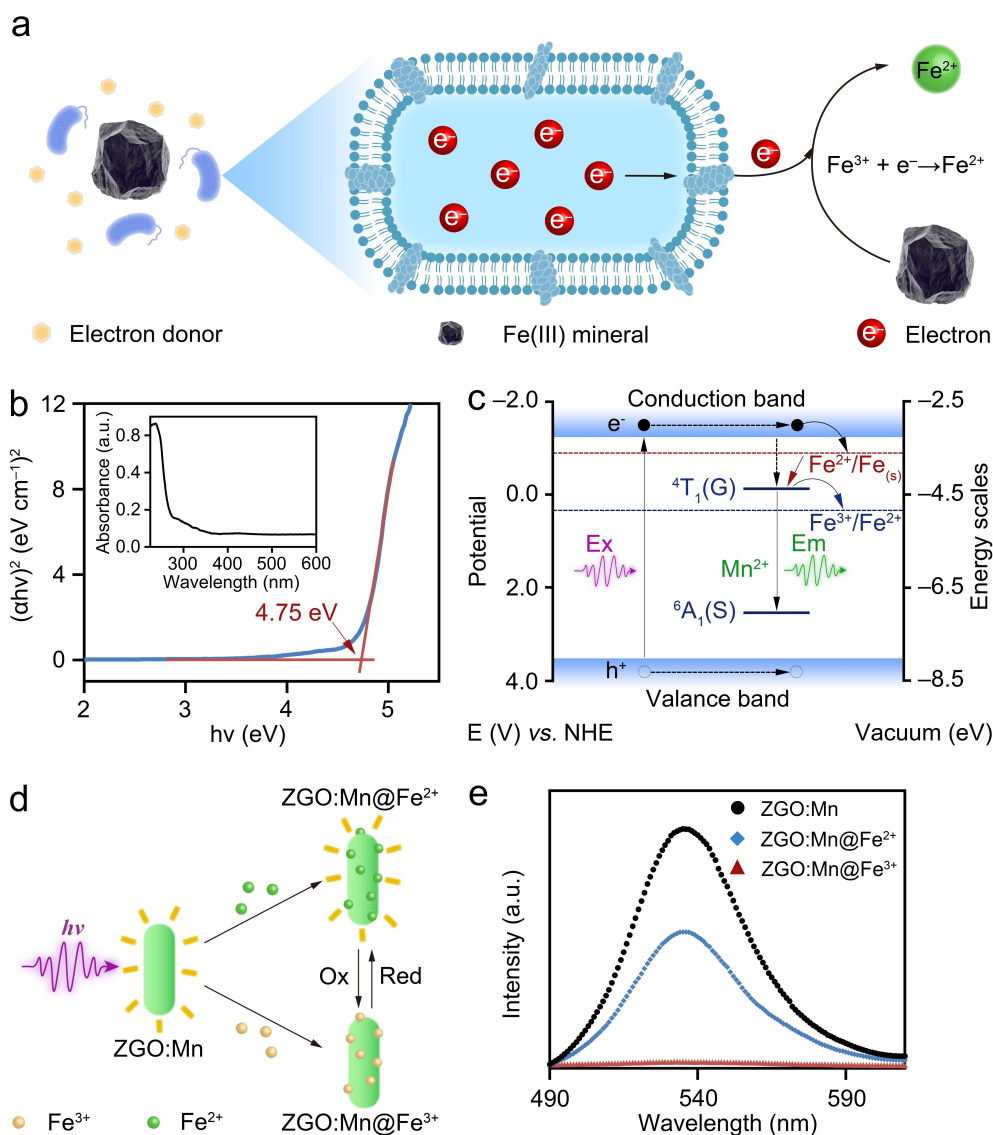

Figure 1. Design of electron-sensing probe. a) Schematic illustration of Fe(III) respiration metabolism in microorganisms. b) Tauc plots of ZGO:Mn nanorods. c) Diagrammatic illustration of photoinduced electron transfer processes between ZGO:Mn nanorods and Fe^{3+}/Fe^{2+}. d) Schematic illustration of ZGO:Mn nanorods upon exposing to redox Fe^{3+}/Fe^{2+} couple. e) Persistent luminescence curves of ZGO:Mn nanorods in response to Fe^{3+} and Fe^{2+}, respectively.

$E_{Fe^{3+},red}$ (−4.80 eV) locates between $^4T_1(G)$ level (−4.36 eV) and $^6A_1(S)$ (−6.67 eV).[17,18c] In this way, photo-excited electrons in $^4T_1(G)$ will be transferred to nearby $E_{Fe^{3+},red}$ instead of relaxing to $^6A_1(S)$,[17,18a,b] and such photoinduced electron transfer would cause persistent luminescence quenching of ZGO:Mn nanorods. In contrast, the Fermi energy level of $E_{Fe^{2+},red}$ (−3.6 eV) locates between conduction band of ZGO:Mn nanorods (−3.24 eV) and the $^4T_1(G)$ level of Mn^{2+} (−4.36 eV). In this case, photo-excited electrons in the conduction band of ZGO:Mn nanorods would transfer to Fermi energy level of $E_{Fe^{2+},red}$ and $^4T_1(G)$ level of Mn^{2+} sequentially, and then relax to $^6A_1(S)$ to emit fluorescence. The difference in persistent luminescence of ZGO:Mn nanorods towards Fe^{3+} and Fe^{2+} might achieve efficient Fe(III) respiration metabolism detection (Figure 1d). To verify this point, the persistent luminescence of ZGO:Mn nanorods in response to Fe^{3+} and Fe^{2+} was investigated. As shown in Figure 1e and Figure S3–5, the persistent luminescence of ZGO:Mn nanorods is quenched by Fe^{3+} efficiently compared with Fe^{2+}. Besides, the persistent luminescence of ZGO:Mn nanorods exhibits negligible variation upon exposure to other physiological relevant metal ions, indicating that ZGO:Mn nanorods display excellent selectivity for Fe^{3+} (Figure S6). The above results indicate that ZGO:Mn nanorods with excellent persistent luminescence performance enable the detection of Fe^{3+}/Fe^{2+} ratio effectively, which might provide a pathway to achieve real-time monitoring of Fe(III) respiration metabolism in microorganism.

Based on the above consideration, we developed a ZGO:Mn@Fe³⁺ probe to monitor Fe(III) respiration metabolism in microorganism (Figure 2a and Figure S7–S11). To explore the capability of ZGO:Mn@Fe³⁺ probe in Fe(III) respiration metabolism monitoring, the ZGO:Mn@Fe³⁺ probe was incubated with *S. putrefaciens* that involves Fe(III) respiration metabolism and *Escherichia coli (E. coli)* without Fe(III) respiration metabolism, respectively. As shown in Figure 2b,c and Figure S12, the persistent luminescence intensity of the ZGO:Mn@Fe³⁺ probe increases with incubation time in *S. putrefaciens* that involves Fe(III) respiration metabolism. In comparison, the ZGO:Mn@Fe³⁺ probe cultured with *E. coli* without Fe(III) respiration metabolism exhibits constant persistent luminescence intensity over time. The above results suggest that the ZGO:Mn@Fe³⁺ probe is specific in microbial Fe(III) respiration metabolism monitoring. It is worth mentioning that the persistent luminescence intensity of ZGO:Mn@Fe³⁺ probe shows negligible change upon incubation with culture supernatant of *S. putrefaciens*, indicating that the metabolite interference exhibits little influence on the ZGO:Mn@Fe³⁺ probe (Figure S13). The ZGO:Mn@Fe³⁺ probe with persistent luminescence could also eliminate the autofluorescence interference in microorganism (Figure S14). The logarithm of persistent luminescence intensity of ZGO:Mn@Fe³⁺ probe linear correlates with the ratio of Fe^{2+}/Fe_{total} (Figure 2d). The limit of detection (LOD) of the ZGO:Mn@Fe³⁺ probe for Fe^{2+} is calculated to be 781 nM according to LOD = 3σ/m, where σ represents the standard deviation of the response and m represents the slope of the
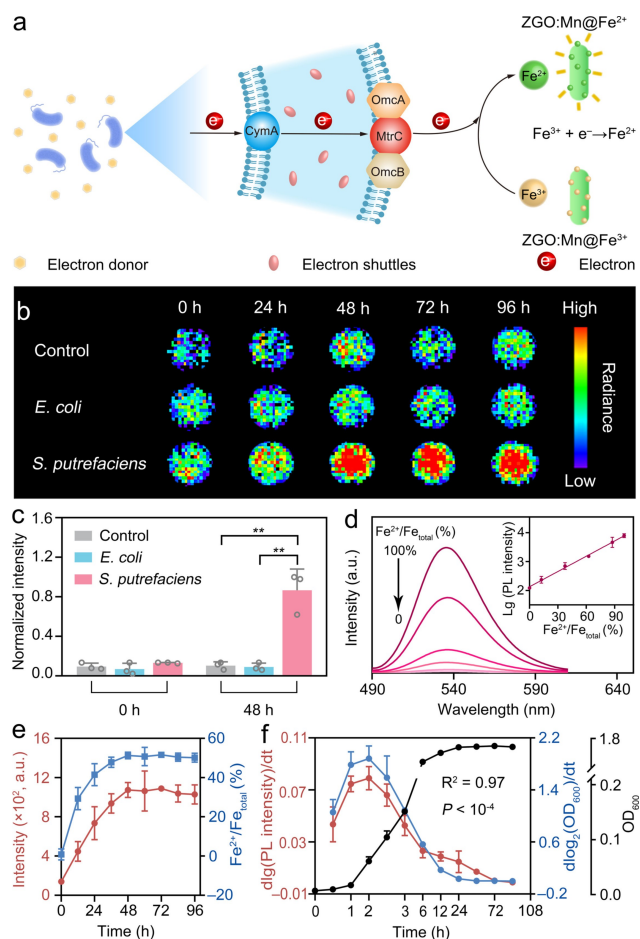

Figure 2. Fe(III) respiration metabolism monitoring. a) Schematic illustration of the monitoring of microbial Fe(III) respiration metabolism with ZGO:Mn@Fe³⁺ probe. b) Persistent luminescence decay images and c) persistent luminescence intensities of the ZGO:Mn@Fe³⁺ probe upon exposure to *S. putrefaciens* and *E. coli*. d) Persistent luminescence curves of ZGO:Mn nanorods in response to different Fe^{2+}/Fe^{3+} ratios with a total Fe concentration of 2.0 mM. Inset: Linear relationship between logarithm of persistent luminescence intensity and Fe^{2+}/Fe_{total} ratio. e) The recorded persistent luminescence intensity of ZGO:Mn@Fe³⁺ probe (red lines) and the calculated Fe^{3+} reduction ratio versus growth time (blue lines) during Fe(III) respiration metabolism in *S. putrefaciens* based on the linear relationship in Figure 2d. f) The derivative of logarithm of persistent luminescence intensity across time (red lines) correlates ($R^2 = 0.97$, $P < 10^{-4}$) with *S. putrefaciens* growth rates (blue lines). Growth rates were measured as the derivative of the logged abundance curve (optical density of culture, black lines).

concentration-dependent response in the Fe(III) respiration metabolism processes (Figure S15).[11a,e,18c] The above results indicate that the ZGO:Mn@Fe³⁺ probe provides a quantitative strategy for Fe(III) respiration metabolism monitoring.

To quantitatively monitor the Fe(III) respiration metabolism in *S. putrefaciens*, the persistent luminescence intensities of ZGO:Mn@Fe³⁺ probe in *S. putrefaciens* over incubation time were recorded (Figure 2e). The Fe^{3+} reduction ratio during the Fe(III) respiration metabolism could be quantified based on the linear relationship between logarithm of persistent luminescence intensity and Fe^{2+}/Fe_{total} ratio in Figure 2d. As indicated in Figure 2e, the

maximal Fe^{2+}/Fe_{total} ratio during the Fe(III) respiration metabolism processes is measured to be about 50%. This value might provide an interpretation for the phenomenon that the natural mineral magnetization shows a stoichiometric magnetite Fe^{2+}/Fe_{total} of 50%. The calculated Fe^{2+}/Fe_{total} ratio is also consistent well with previous studies,[9a] demonstrating that the ZGO:Mn@Fe^{3+} probe is capable to monitor Fe(III) respiration metabolism. Bacterial colonies after 96 h incubation (2.16×10^9 CFU mL^{-1} for bare *S. putrefaciens*, 1.91×10^9 CFU mL^{-1} for ZGO:Mn-*S. putrefaciens*, and 1.97×10^9 CFU mL^{-1} for ZGO:Mn@Fe^{3+}-*S. putrefaciens*) are detected on substrate, indicating that both the ZGO:Mn nanorods and the ZGO:Mn@Fe^{3+} probe exhibit low toxicity against *S. putrefaciens* (Figure S16). Besides, the ZGO:Mn@Fe^{3+} probe remains stable after 4 days co-culture with *S. putrefaciens* (Figure S17). The negligible change of persistent luminescence of ZGO:Mn@Fe^{3+} probe during the whole incubation processes in medium solution also verifies the excellent stability of ZGO:Mn@Fe^{3+} probe (Figure S18). Previous studies have indicated that the metabolic activities of microorganism are highly correlated to the metabolic status.[19] The relationship between the persistent luminescence intensity of ZGO:Mn@Fe^{3+} probe and bacterial growth rates was plotted in Figure 2f. As shown in Figure 2f, the derivative of logarithm of persistent luminescence intensity across time correlates well with the bacterial growth rates ($R^2 = 0.97$, $P < 10^{-4}$) that was calculated as the derivative of bacterial abundance ($\log_2 OD_{600}$) across time.[19a,20] The above results suggest that ZGO:Mn@Fe^{3+} probe could offer real-time and quantitative insights in complex microbial Fe(III) respiration metabolism monitoring.

Besides the capability for real time detection of Fe(III) respiration metabolism in microorganism, ZGO:Mn@Fe^{3+} probe could also facilitate the exploration of relevant biomolecules that are involved in microbial metabolism. Genetic studies have revealed that CymA, MtrC, OmcA and OmcB are involved in the electron transfer processes of bacteria.[16a,21] CymA is a key membrane-anchor protein that could transfer electrons from cytoplasm to periplasm in *S. putrefaciens*.[22] MtrC, OmcA and OmcB on the bacteria surface could transfer electrons to minerals directly.[23] Mutants with CymA-encoding gene deleted ($\Delta CymA$) and MtrC-encoding gene deleted ($\Delta MtrC$) were constructed to investigate the role of CymA and MtrC in electron transfer processes, respectively (Figure S19 and S20). As shown in Figure 3a–c, the recovery rates of persistent luminescence in both $\Delta CymA$ and $\Delta MtrC$ mutants are slower than wild-type *S. putrefaciens*, indicating that the Fe(III) respiration metabolism is impeded in the absence of CymA or MtrC. The OmcA and OmcB inhibitor vanadate (V_2O_5) was employed to verify the role of OmcA and OmcB in Fe(III) respiration metabolism.[24] As shown in Figure 3d, the persistent luminescence of ZGO:Mn@Fe^{3+} probe in *S. putrefaciens* increases slowly in the presence of V_2O_5, and the luminescence intensity exhibits a dose-dependent behavior in response to V_2O_5 (Figure S21). This phenomenon suggests that the electrons transfer pathways were impeded once OmcA and OmcB were blocked. Recently, flavin
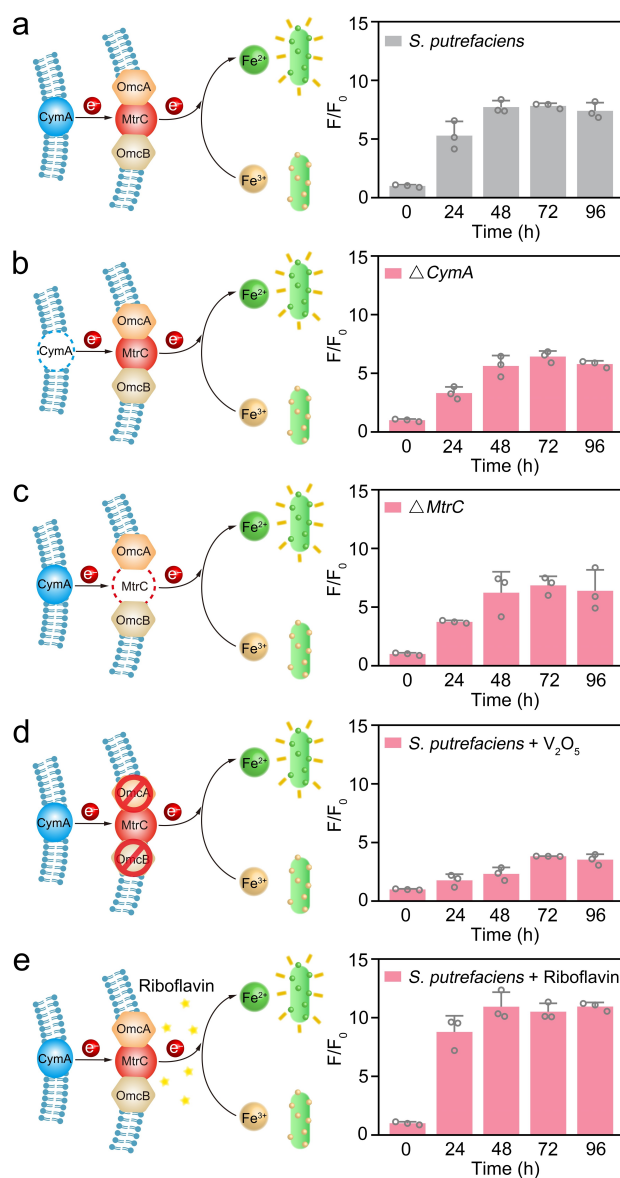

Figure 3. Metabolism mechanism verification. Schematic and persistent luminescence intensity of the ZGO:Mn@Fe^{3+} probe co-cultured with a) wild-type *S. putrefaciens*, b) $\Delta CymA$ mutants and c) $\Delta MtrC$ mutants. Schematic and persistent luminescence intensity of the ZGO:Mn@Fe^{3+} probe upon the addition of d) V_2O_5 inhibitor and e) electron transfer shuttle riboflavin.

shuttles have been proved to mediate electron transfer to extracellular acceptors through conjunction with extracellular flavoprotein.[16b,25] The electrons transfer ability of flavin was also investigated with ZGO:Mn@Fe^{3+} probe. After the addition of flavin shuttles such as riboflavin, flavin adenine dinucleotide (FAD) and flavin mononucleotide (FMN), the persistent luminescence intensity of ZGO:Mn@Fe^{3+} probe in *S. putrefaciens* increases by 41.5%, 31.4% and 24.3%% after 48 h incubation (Figure 3e and Figure S22, S23). It is worth mentioning that exogenous substances such as V_2O_5 and riboflavin show negligible interference on the persistent luminescence of ZGO:Mn@Fe^{3+} probe (Figure S24). These results confirm the critical role of CymA, MtrC, OmcA,

Angew. Chem. Int. Ed. **2022**, e202115572 (4 of 8)

© 2022 Wiley-VCH GmbH

OmcB and flavin shuttles in transferring cytoplasm electrons to extracellular acceptors in Fe(III) respiration metabolism. Also, the above investigations clearly indicate that the ZGO:Mn@Fe^{3+} probe is capable of exploring the role of related biomolecules in microbial Fe(III) respiration metabolism.

Microbial metabolism in nature are complex due to particularly complicated metabolism environment and dynamic processes.[26] Typically, bacteria encounter a myriad of stresses in nature, and it would generate a series of adaptive and protective responses to adapt external environment.[27] To explore the capability of ZGO:Mn@Fe^{3+} probe for Fe(III) respiration metabolism monitoring in complicated environment, the persistent luminescence of ZGO:Mn@Fe^{3+} probe co-cultured with *S. putrefaciens* under environmental stress stimulus was investigated. Figure 4a presents the Fe(III) respiration metabolism of *S. putrefaciens* in response to oxygen-stress. When oxygen was injected into the ZGO:Mn@Fe^{3+} probe and *S. putrefaciens* co-culture solution, the persistent luminescence quenched immediately, while the persistent luminescence intensity in control group without *S. putrefaciens* remains stable. The quenched luminescence can be ascribed to the oxidation of Fe^{2+} to Fe^{3+} by oxygen. Then, the persistent luminescence of ZGO:Mn@Fe^{3+} probe gradually recovers to the original intensity, suggesting that the injected oxygen was consumed by *S. putrefaciens* and Fe^{3+} was reduced to Fe^{2+} through Fe(III) respiration metabolism (Figure S25). When the culture temperature elevates from 303 K to 310 K, the persistent luminescence recovery rate decreases, suggesting that the increase of temperature impedes the Fe(III) respiration metabolism in *S. putrefaciens* (Figure 4b and Figure S26). The impeded metabolism at 310 K is partially due to reduced metabolic status or enzymatic activity in the electron transfer chains. The stress response detecting capability of ZGO:Mn@Fe^{3+} probe provides a facile strategy for stress-tolerant strains metabolic activity monitoring.

Besides the influence of natural environmental stress, interactions among microorganism also play key roles in microbial metabolism. By trading metabolites, exchanging signals or integrating pathways, microbial co-culture coordinates specific activities, thus determining the stability, functionality and dynamics of communities.[28] For example, *E. coli-S. cerevisiae* microbial co-culture can work cooperatively by integrating relevant metabolic pathways of *E. coli* and *S. cerevisiae* to improve paclitaxel biomanufacturing efficiency.[29] In microbial co-culture of *Rhodopseudomonas palustris* TIE-1 (*R. palustris*)-*S. putrefaciens*, *S. putrefaciens* could provide Fe^{2+} electron donor for phototrophic *R. palustris* through Fe(III) respiration metabolism.[9b] Furthermore, Fe^{2+} can be oxidized to Fe^{3+} by *R. palustris* under light illumination.[9b] The confocal images in Figure 5a and Figure S27 show the morphologies of glutaraldehyde-fixed *R. palustris* (blue) and *S. putrefaciens* (red) in *R. palustris-S.*
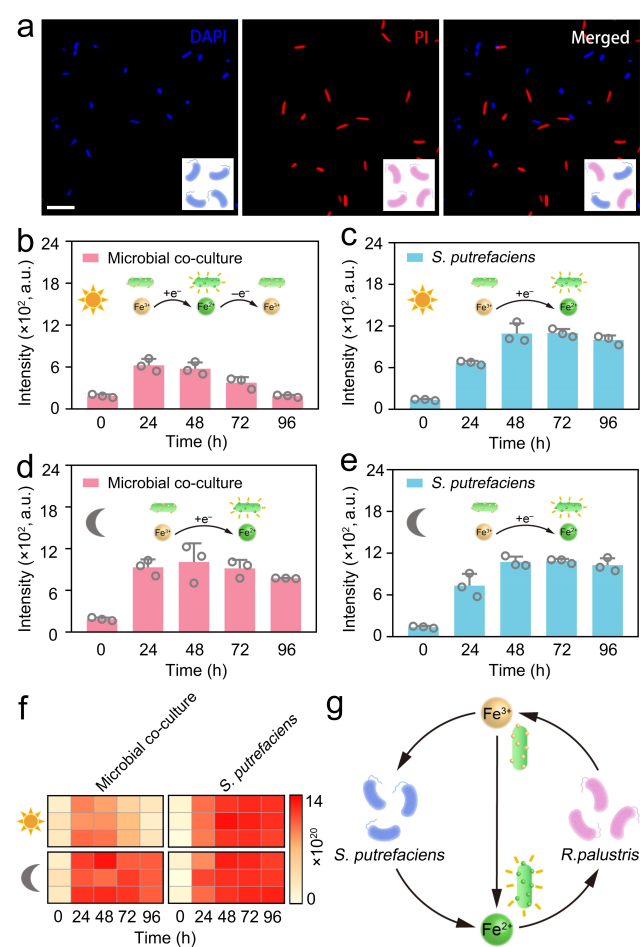
Figure 5. Metabolism monitoring in microbial co-culture. a) Confocal fluorescence imaging of *R. palustris* (DAPI, blue) and *S. putrefaciens* (PI, red) in microbial co-culture. Monitoring of metabolism in b) microbial co-culture and c) *S. putrefaciens* with ZGO:Mn@Fe^{3+} probe under light illumination. Monitoring of metabolism in d) microbial co-culture and e) *S. putrefaciens* with ZGO:Mn@Fe^{3+} probe in the dark. f) The number of electrons transferred to ZGO:Mn@Fe^{3+} probe under different conditions, $n = 3$. g) Schematic of ZGO:Mn@Fe^{3+} probe for the monitoring of Fe redox cycling metabolism in *R. palustris-S. putrefaciens* co-culture.
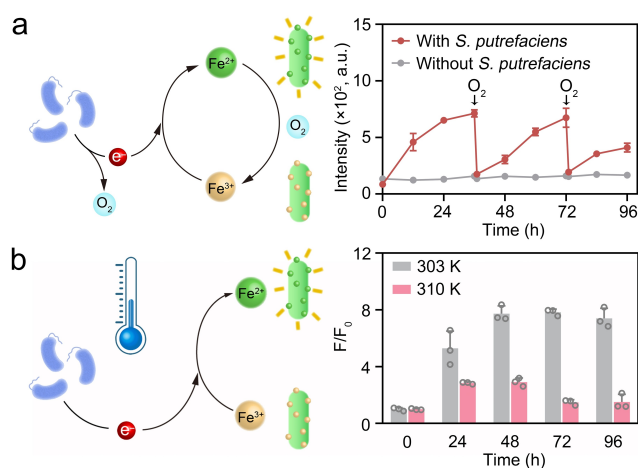

Figure 4. Dynamic stress responses monitoring. a) Oxygen-stress and b) temperature-stress Fe(III) respiration metabolism monitored with ZGO:Mn@Fe^{3+} probe.

Angew. Chem. Int. Ed. **2022**, e202115572 (5 of 8)

© 2022 Wiley-VCH GmbH

putrefaciens co-culture. To monitor the Fe redox cycling metabolism existed in *R. palustris*-*S. putrefaciens* co-culture, the ZGO:Mn@Fe^{3+} probe was incubated with *R. palustris*-*S. putrefaciens* co-culture and the persistent luminescence performance was recorded. To give a clear comparison, pure *S. putrefaciens* was selected as the control. In Figure 5b and Figure 5c, it can be observed that the persistent luminescence intensities of ZGO:Mn@Fe^{3+} probe in *R. palustris*-*S. putrefaciens* co-culture under light illumination are much lower compared with that of bare *S. putrefaciens* at different growth stages. The amounts of *S. putrefaciens* in Figure 5b and 5c are further investigated with the corresponding fluorescence in situ hybridization (FISH) probe of *S. putrefaciens*.[30] Flow cytometric analysis shows that the *S. putrefaciens* amounts in *R. palustris*-*S. putrefaciens* co-culture and bare *S. putrefaciens* under light illumination are nearly consistent at the same growth stages (Figure S28 and Table S3). Hence, the decreased luminescence in Figure 5b suggests that the Fe redox cycling occurred in the microbial co-culture under light illumination. By contrast, the *R. palustris*-*S. putrefaciens* co-culture in dark shows similar persistent luminescence intensity compared with bare *S. putrefaciens* (Figure 5d, e). This phenomenon suggests that Fe redox cycling in microbial co-culture under dark environment is hindered, and the impeded Fe redox cycling is due to the absence of Fe^{2+}→Fe^{3+} conversion in phototrophic *R. palustris* in dark. The luminescence performance variation indicates that Fe redox cycling metabolism in microbial co-culture could be effectively monitored by ZGO:Mn@Fe^{3+} probe. Meanwhile, the culture solution of *R. palustris*-*S. putrefaciens* under light irradiation turned purplish red rapidly (Figure S29), indicating that the growth rate of *R. palustris* in microbial co-culture was accelerated compared with bare *R. palustris*. The synergistic mutualism between *S. putrefaciens* and *R. palustris* under light irradiation promotes the metabolites exchange and *R. palustris* growth. The number of electrons transferred to ZGO:Mn@Fe^{3+} probe in *R. palustris*-*S. putrefaciens* microbial co-culture and bare *S. putrefaciens* can be calculated based on the following equation:

$$N = n_{Fe^{2+}} \times N_A \tag{1}$$

where *N* represents electron transfer numbers, and $n_{Fe^{2+}}$ represents the mole number of Fe^{2+}. N_A is Avogadro constant (6.02×10^{23}). Figure 5f summarizes the electron transfer numbers in microbial co-culture and bare *S. putrefaciens* cultured at different growth stages. The calculated electron transfer number from *R. palustris*-*S. putrefaciens* co-culture to ZGO:Mn@Fe^{3+} probe is less than that of *S. putrefaciens*. The decreased electrons transfer number in *R. palustris*-*S. putrefaciens* co-culture can be attributed to the existence of Fe redox cycling between *S. putrefaciens* and *R. palustris* (Figure 5g). The above results indicate that ZGO:Mn@Fe^{3+} probe provides a robust analytical tool for Fe redox cycling metabolism monitoring in microbial co-culture.

R. palustris was reported as a microbial host for lycopene production.[31] As illustrated in Figure 6a, lycopene is
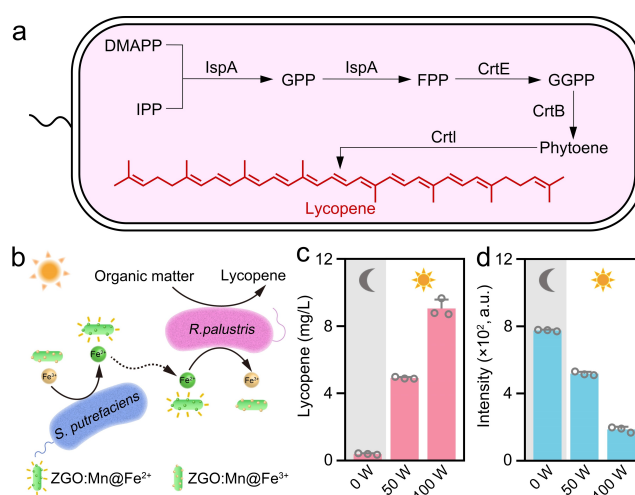
Figure 6. Metabolism monitoring to guide biosynthesis efficiency. a) Lycopene biosynthesis pathways in *R. palustris* (GPP, geranyl pyrophosphate; FPP, farnesyl pyrophosphate; GGPP, geranylgeranyl pyrophosphate; IspA, farnesyl pyrophosphate synthase; CtrE, a forme of GGPP synthase; CtrB, phytoenesynthase; Ctrl, phytoene desaturase). b) Schematic illustration of the monitoring of lycopene biosynthesis process in microbial co-culture with ZGO:Mn@Fe^{3+} probe. c) Persistent luminescence intensity of ZGO:Mn@Fe^{3+} probe in microbial co-culture under different light irradiations. d) Lycopene biosynthesis efficiency in microbial co-culture under different light irradiations.

naturally produced by the condensation of isopentenyl diphosphate (IPP) and dimethylallyl diphosphate (DMAPP) through carotenoid biosynthetic pathway in *R. palustris*. The *R. palustris*-*S. putrefaciens* microbial co-culture with different bacteria ratios under light irradiation all show improved lycopene biosynthesis efficiency compared with bare *R. palustris* (Figure S30), and the improved biosynthesis efficiency coincidences with accelerated Fe redox cycling metabolism in microbial co-culture. Consequently, the monitoring of Fe redox cycling in *R. palustris*-*S. putrefaciens* co-culture might guide the lycopene biosynthetic process optimization (Figure 6b). To this end, we investigated the relationship between persistent luminescence of ZGO: Mn@Fe^{3+} probe and lycopene yield in *R. palustris*-*S. putrefaciens* co-culture under different light irradiations. Figure 6c shows that with the increase of light irradiation, the persistent luminescence intensity of ZGO:Mn@Fe^{3+} probe decreases while the lycopene yield improves (Figure 6d). The improved lycopene yield originates from the accelerated Fe redox cycling metabolism in *R. palustris*-*S. putrefaciens* co-culture with high dose of light irradiation. The correlation between the persistent luminescence intensity and lycopene yield demonstrated that the ZGO: Mn@Fe^{3+} probe could be utilized to monitor microbial co-culture metabolism process to guide biosynthesis efficiency optimization.

Conclusion

In summary, we developed an electron-sensing probe ZGO:$Mn@Fe^{3+}$ for real-time monitoring of Fe(III) respiration metabolism in microorganism. The critical roles of CymA, MtrC, OmcA, OmcB and flavin in transferring cytoplasm electrons to extracellular acceptors during the Fe(III) respiration metabolism were validated with the ZGO:$Mn@Fe^{3+}$ probe. The electron-sensing probe ZGO:$Mn@Fe^{3+}$ could also be utilized to track the metabolic response of *S. putrefaciens* to environmental stress and metabolic processes involved in microbial co-culture. Moreover, the electron-sensing probe ZGO:$Mn@Fe^{3+}$ could be a guide for microbial co-culture biosynthesis conditions optimization. The design of electron-sensing probes by coupling related metabolites and luminescence nanomaterials proposes a general strategy for relevant metabolism processes monitoring.

Acknowledgements

Conflict of Interest

The authors declare no conflict of interest.

Data Availability Statement

The data that support the findings of this study are available in the supplementary material of this article.

[1] V. Chubukov, L. Gerosa, K. Kochanowski, U. Sauer, *Nat. Rev. Microbiol.* **2014**, *12*, 327–340.
[2] a) D. A. Hutchins, F. X. Fu, *Nat. Microbiol.* **2017**, *2*, 17058; b) H. Yu, J. R. Leadbetter, *Nature* **2020**, *583*, 453–458.
[3] a) A. S. Khalil, J. J. Collins, *Nat. Rev. Genet.* **2010**, *11*, 367–379; b) J. M. Clomburg, A. M. Crumbley, R. Gonzalez, *Science* **2017**, *355*, aag0804.
[4] W. B. Black, L. Y. Zhang, W. S. Mak, S. Maxel, Y. T. Cui, E. King, B. Fong, A. S. Martinez, J. B. Siegel, H. Li, *Nat. Chem. Biol.* **2020**, *16*, 87–94.
[5] a) S. Cheong, J. M. Clomburg, R. Gonzalez, *Nat. Biotechnol.* **2016**, *34*, 556–561; b) C. Liang, J. P. Schimel, J. D. Jastrow, *Nat. Microbiol.* **2017**, *2*, 17105.
[6] F. Beaufay, J. Coppine, R. Hallez, *Curr. Opin. Microbiol.* **2021**, *60*, 104–113.
[7] J. D. Winkler, K. Erickson, A. Choudhury, A. L. Halweg-Edwards, R. T. Gill, *Curr. Opin. Biotechnol.* **2015**, *36*, 107–114.
[8] a) Y. F. Zhang, S. Tsitkov, H. Hess, *Nat. Catal.* **2018**, *1*, 276–281; b) N. Z. Guan, J. H. Li, H. D. Shin, G. C. Du, J. Chen, L. Liu, *Appl. Microbiol. Biotechnol.* **2017**, *101*, 3991–4008.
[9] a) S. Glasauer, S. Langley, T. J. Beveridge, *Science* **2002**, *295*, 117–119; b) J. M. Byrne, N. Klueglein, C. Pearce, K. M. Rosso, E. Appel, A. Kappler, *Science* **2015**, *347*, 1473–1476; c) K. A. Weber, L. A. Achenbach, J. D. Coates, *Nat. Rev. Microbiol.* **2006**, *4*, 752–764.
[10] a) Z. Yan, P. Joshi, C. A. Gorski, J. G. Ferry, *Nat. Commun.* **2018**, *9*, 1642; b) C. F. Gan, R. R. Wu, Y. S. Luo, J. H. Song, D. Z. Luo, B. Li, Y. G. Yang, M. Y. Xu, *Appl. Environ. Microbiol.* **2020**, *87*, e02192-20.
[11] a) B. Sui, S. Tang, T. Liu, B. Kim, K. D. Belfield, *ACS Appl. Mater. Interfaces* **2014**, *6*, 18408–18412; b) H. Bischof, S. Burgstaller, M. Waldeck-Weiermair, T. Rauter, R. Malli, *Cells* **2019**, *8*, 492; c) H. Liu, X. Li, M. Wang, X. Chen, X. Su, *Anal. Chim. Acta* **2017**, *990*, 150–156; d) P. Lv, Y. X. u, Z. Liu, G. Li, B. Ye, *Microchem. J.* **2020**, *152*, 104255; e) X. Y. Zhu, Y. Duan, P. Li, H. M. Fan, T. Y. Han, X. N. Huang, *Anal. Methods* **2019**, *11*, 642–647.
[12] a) L. Q. Li, Z. H. Liu, *J. Fluoresc.* **2017**, *27*, 427–431; b) K. Dayanidhi, N. S. Eusuff, *New J. Chem.* **2021**, *45*, 9936–9943; c) K. Inoue, S. Aikawa, S. Masaru, Y. Fukushima, *J. Inclusion Phenom. Macrocyclic Chem.* **2018**, *91*, 171–177; d) Z. Q. Yan, Y. J. Zhu, J. Xu, C. Wang, Y. Y. Zheng, P. Y. Li, L. Hu, J. M. You, *Anal. Methods* **2017**, *9*, 6240–6245.
[13] a) K. Dutta, S. Panda, *J. Electrochem. Soc.* **2018**, *165*, B378–B389; b) L. Norocel, G. Gutt, *Aust. J. Grape Wine Res.* **2019**, *25*, 161–164; c) A. Ooi, E. Tada, A. Nishikata, *J. Electrochem. Soc.* **2016**, *163*, F1558–F1563.
[14] P. Y. Lv, Y. Y. Xu, Z. Liu, G. P. Li, B. X. Ye, *Microchem. J.* **2020**, *152*, 104255.
[15] J. Wang, Q. Q. Ma, W. Zheng, H. Y. Liu, C. Q. Yin, F. B. Wang, X. Y. Chen W H Tan, *ACS Nano* **2017**, *11*, 8185–8191.
[16] a) L. Shi, H. L. Dong, G. Reguera, H. Beyenal, A. H. Lu, J. Liu, H. Q. Yu, J. K. Fredrickson, *Nat. Rev. Microbiol.* **2016**, *14*, 651–662; b) E. Marsili, D. B. Baron, I. D. Shikhare, D. Coursolle, J. A. Gralnick, D. R. Bond, *Proc. Natl. Acad. Sci. USA* **2008**, *105*, 3968–3973.
[17] F. F. Chi, X. T. Wei, B. Jiang, Y. H. Chen, C. K. Duan, M. Yin, *Dalton Trans.* **2018**, *47*, 1303–1311.
[18] a) Y. H. Jin, Y. H. Hu, H. Duan, L. Chen, X. J. Wang, *RSC Adv.* **2014**, *4*, 11360–11366; b) Y. Cong, Y. Y. He, B. Dong, Y. Xiao, L. M. Wang, *Opt. Mater.* **2015**, *42*, 506–510; c) N. Li, A. Than, C. C. Sun, J. Q. Tian, J. Chen, K. Y. Pu, X. C. Dong, P. Chen, *ACS Nano* **2016**, *10*, 11475–11482.
[19] a) L. Y. Lin, J. Song, Y. H. Du, Q. Y. Wu, J. Gao, Y. L. Song, C. Y. Yang, W. Wang, *Angew. Chem. Int. Ed.* **2020**, *59*, 11923–11926; *Angew. Chem.* **2020**, *132*, 12021–12024; b) S. O. Kelley, *SLAS Technol.* **2017**, *22*, 113–121.
[20] a) T. Korem, D. Zeevi, J. Suez, A. Weinberger, T. Avnit-Sagi, M. Pompan-Lotan, E. Matot, G. Jona, A. Harmelin, N. Cohen, A. Siroto-Madi, C. A. Thaiss, M. Pevsner-Fischer, R. Sorek, R. Xavier, E. Elinav, E. Segal, *Science* **2015**, *349*, 1101–1106; b) L. M. Blank, U. Sauer, *Microbiology* **2004**, *150*, 1085–1093.
[21] G. Fan, A. J. Graham, J. Kolli, N. A. Lynd, B. K. Keitz, *Nat. Chem.* **2020**, *12*, 638–646.
[22] S. Xu, A. Barrozo, L. M. Tender, A. I. Krylov, M. Y. El-Naggar, *J. Am. Chem. Soc.* **2018**, *140*, 10085–10089.
[23] X. X. Jing, Y. C. Wu, L. Shi, C. L. Peacock, N. M. Ashry, C. H. Gao, Q. Y. 642, P. Cai, *Appl. Environ. Microbiol.* **2020**, *86*, e01941–20.

Angew. Chem. Int. Ed. **2022**, e202115572 (7 of 8)

© 2022 Wiley-VCH GmbH

[24] J. Borloo, B. Vergauwen, L. D. Smet, A. Brig, B. Motte, B. Devreese, J. V. Beeumen, *FEBS J.* **2007**, *274*, 3728–3738.

[25] a) Y. Yang, Y. Z. Ding, Y. D. Hu, B. Cao, S. A. Rice, S. Kjelleberg, H. Song, *ACS Synth. Biol.* **2015**, *4*, 815–823; b) S. H. Light, L. Su, R. Rivera-Lugo, J. A. Cornejo, A. Louie, A. T. Iavarone, C. M. Ajo-Franklin, D. A. Portnoy, *Nature* **2018**, *562*, 140–144; c) N. J. Kotloski, J. A. Gralnick, *mBio* **2013**, *4*, e00553-12.

[26] E. Abatenh, B. Gizaw, Z. Tsegaye, M. Wassie, *Open J. Environ. Microbiol.* **2017**, *1*, 038–046.

[27] C. Y. Bonilla, *Integr. Comp. Biol.* **2020**, *60*, 126–133.

[28] a) H. W. Zhu, H. K. Meng, W. Zhang, H. C. Gao, J. Zhou, Y. P. Zhang, Y. Li, *Nat. Commun.* **2019**, *10*, 4282; b) H. Y. Lu, J. C. Villada, P. K. H. Lee, *Trends Biotechnol.* **2019**, *37*, 152–166.

[29] a) Y. Liu, M. Z. Ding, W. Ling, Y. Yang, X. Zhou, B. Z. Li, T. Chen, Y. Nie, M. X. Wang, B. X. Zeng, *Energy Environ. Sci.* **2017**, *10*, 1600–1609; b) H. Song, M. Z. Ding, X. Q. Jia, Q. Ma, Y. J. Yuan, *Chem. Soc. Rev.* **2014**, *43*, 6954–6981; c) K. Zhou, K. J. Qiao, S. Edgar, G. Stephanopoulos, *Nat. Biotechnol.* **2015**, *33*, 377–383.

[30] a) R. Almstrand, D. M. Drennan, J. O. Sharp, *J. Basic Microbiol.* **2015**, *55*, 798–802; b) L. J. Tan, H. H. Li, B. W. Chen, J. M. Huang, Y. F. Li, H. M. Zheng, H. Q. Liu, Y. Zhao, J. J. Wang, *Food Control* **2021**, *125*, 207983; c) S. Van Nevel, S. Koetzsch, C. R. Proctor, M. D. Besmer, E. I. Prest, J. S. Vrouwenvelder, A. Knezev, N. Boon, F. Hammes, *Water Res.* **2017**, *113*, 191–206.

[31] M. J. Li, Q. Q. Xia, H. B. Zhang, R. B. Zhang, J. M. Yang, *J. Agric. Food Chem.* **2020**, *68*, 14104–14122.

Research Articles

Real-Time Monitoring of Dynamic Microbial Fe(III) Respiration Metabolism with a Living Cell-Compatible Electron-Sensing Probe
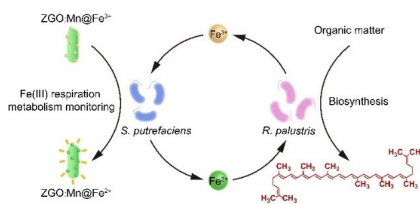
An electron-sensing probe Zn_2GeO4:Mn@Fe^{3+} was developed to achieve dynamic Fe(III) respiration metabolism monitoring in *S. putrefaciens*. With excellent monitoring performance, the Zn_2GeO4:Mn@Fe^{3+} probe offers the potential to track the dynamic Fe(III) respiration metabolic response of *S. putrefaciens* to environmental stress and microbial co-culture interactions. Additionally, the Zn_2GeO4:Mn@Fe^{3+} probe provides guidance for biosynthesis efficiency optimization.